THE JOURNAL OF PHYSICAL CHEMISTRY B

Article

pubs.acs.org/JPCB

Application of the Multi-Step EPD Technique to Fabricate Thick TiO_2 Layers: Effect of Organic Medium Viscosity on the Layer Microstructure

A. A. Sadeghi, T. Ebadzadeh, B. Raissi,* S. Ghashghaie, and S. M. A. Fateminia

Materials & Energy Research Centre, P.O. Box 31787/316, Alborz, Iran

ABSTRACT: In the present study, electrophoretic deposition (EPD) was used to obtain dense layers of TiO_2 in four organic media—methanol, ethanol, 1-propanol, and butanol—with different TiO_2 nanoparticle concenterations of 1−8 g/L. Microstructural study of the obtained layers by scanning electron (SEM) and optical microscope (OM) revealed that the multistep EPD technique could effectively prevent crack formation across the layer compared with the single-step method and will consequently increase the critical cracking thickness (CCT). The quality of EPD layers was also affected by viscosity. According to SEM and atomic force microscope (AFM) results, as the viscosity of the medium increased, more compact layers were formed which can be attributed to the lower deposition rates in heavier alcohols. High deposition rate in methanol and ethanol was also confirmed by zeta potential results. Suspension viscosity was interestingly observed to control the threshold concentration above which crack formation would occur. These values were measured to be 3 and 5 g/L for methanol and ethanol, respectively. However, in suspensions based on more viscous alcohols, the threshold concentration increased to 8 g/L which implied the decisive role of medium on concentration limits. It indicates that by employing organic vehicles of higher viscosity it is possible to maintain the CCT values obtained in less viscous media with no need to decrease the colloidal concentration of the suspension.

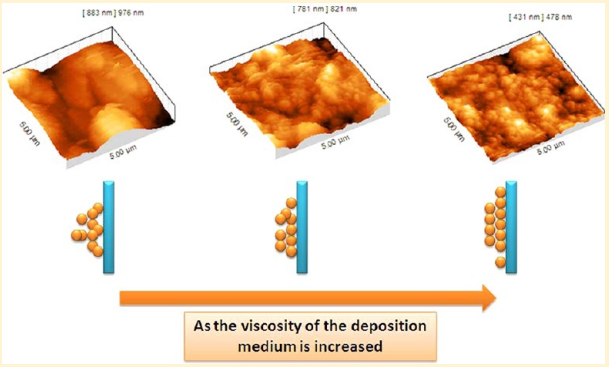

1. INTRODUCTION

Titanium dioxide (TiO_2) is an important wide band gap semiconductor that exists in three crystalline structures: tetragonal anatase, tetragonal rutile, or orthorhombic brookite.[1] TiO_2 has attracted considerable interest due to its unique physical and chemical properties such as large energy gap (3.0 eV rutile, 3.2 eV anatase),[2] high refractive index,[3] and high dielectric constant.[4] TiO_2 has been widely used as a photocatalyst,[5] dye sensitized solar cell (DSSC) film,[6] gas sensor,[7] and protective coating.[8] The TiO_2 based layers have also been employed in biomaterials-related applications such as implants.[9] In most industrial applications of TiO_2, crack-free thick or thin films with a uniform microstructure are required. In order to obtain such high quality levels, numerous methods such as sputtering,[10] sol gel,[11] doctor blade,[12] screen printing,[13] plasma spray,[14] atomic layer deposition,[15] and chemical vapor deposition[16] have been employed. In addition to these techniques, electrophoretic deposition (EPD) has been widely employed as a simpler and cheaper route that makes it possible to obtain reliable ceramic thick films.

EPD is a colloidal process wherein ceramic bodies are shaped directly by applying a DC electric field to a stable colloidal suspension. In practice, EPD is a combination of two processes: (i) electrophoresis, which is the motion of charged particles in suspension under the application of an electric field, and (ii) deposition, defined as the coagulation of particles into a dense mass.[17] In order to apply this technique, it is essential to produce a stable suspension containing charged particles (high zeta-potential) freely moving across the medium. The main parameters concerning the suspension are the particle concentration, size distribution, conductivity, and pH as well as the viscosity of the medium.[18]

Although electrophoretic deposition of TiO_2 in aqueous media has been extensively described in the literature,[19] the use of water-based suspensions causes a number of problems such as electrolysis of water that occurs even at low voltages (~5 V) and leads to gaseous emission of H_2 or O_2 at the collecting electrode. Gas bubbles can cause defects within the microstructure of the deposited layer.[18,20] Considering these challenges, organic liquids are generally preferred to water in EPD processes.

Although organic media have been successfully used for the preparation of stable colloidal suspensions and subsequent deposition of particles under the application of an electric field, few researchers have investigated the effect of organic medium characteristics on the deposition microstructure. Panigrahi et al.

Special Issue: Electrophoretic Deposition

Received: July 13, 2012
Revised: December 29, 2012
Published: January 3, 2013

   dx.doi.org/10.1021/jp306976p | *J. Phys. Chem. B* 2013, 117, 1731−1737

studied the electrophoretic deposition of doped ceria in various nonaqueous solvents. They obtained uniform deposits in butanol as a viscous medium, while a porous microstructure was achieved in acetyl acetone.[21] Such effects have also been observed in alternating fields where we discussed the effect of acetone and isopropanol on the low-frequency electrophoretic deposition pattern of ZnO nanoparticles. We obtained two different patterns and attributed it to suspension parameters such as viscosity, conductivity, particle size distribution, and diffusion coefficient.[22] Dor et al. prepared mesoporous TiO_2 layers by EPD and measured the density of the obtained layers as a function of organic medium. They concluded that the deposition rate could be varied by changing the particle concentration and proper choice of the solvent.[23] In another study, Grinis et al. fabricated DSSC photolelectrodes by electrophoretic deposition of TiO_2 in alcoholic media and observed that cells fabricated from lower concentration suspensions showed higher efficiencies. They concluded that the intensification of TiO_2 particle agglomeration in the more concentrated suspensions would result in a poor packing density of the electrophoretically deposited films.[24]

In this paper, which is mainly focused on obtaining crack-free layers for future DSSC applications, we investigated the effect of four different organic-based TiO_2 suspensions—methanol, ethanol, 1-propanol, and butanol—on the microstructure of the electrophoretically deposited layers. We successfully avoided crack formation across the deposited layers to increase the CCT value by using a multistep EPD technique instead of the conventional single-step method. Then, the role of organic media of higher viscosity on preventing crack formation at high particle concentrations was studied.

2. EXPERIMENTAL SECTION

2.1. Materials. Titanium dioxide nanopowder (Degussa P25) composed of 30% rutile and 70% anatase, with a BET surface area of 50 m^2/g and an average primary particle size of 21 nm, was used as the starting material. The organic solvents—methanol, ethanol, 1-propanol, and butanol—were purchased from Merck and used as received without any further purification. Two copper substrates with an area of about 4.5 cm^2 (3 cm × 1.5 cm) were used as the anode and cathode.

2.2. Electrophoretic Deposition (EPD). The four suspensions containing TiO_2 nanoparticles with concentrations of 1, 2, 3, 4, 5, 6, 7, and 8 g/L for each organic medium were prepared without the addition of any surfactants. Each suspension was first sonicated for 15 min and then magnetically stirred for 24 h at 400 rpm. The prepared suspensions were then sonicated for 15 min to break up the remaining agglomerates.

Electrophoretic deposition was carried out at a constant voltage of 50 V using a regulated DC power supply (EICO 1030) and an anode-to-cathode distance of 1 cm. The substrates were washed in distilled water and acetone and finally dried in air for 15 min. The relation between powder concentration and deposited mass in each medium was obtained at different concentrations (1−8 g/L) and a constant deposition duration of 3 min (6 × 30 s).

For the EPD process of TiO_2 nanoparticles, a multistep deposition technique was employed while the recycle process consisted of simple drying at 150 °C at the end of each step. In order to evaluate the deposition rate, the process was carried out at different time intervals of 30, 60, 90, 120, 150, and 180 s employing a constant applied voltage of 50 V.

After drying, the deposition pattern of the obtained layers was studied using optical microscope (OM, Olympus/BX61), atomic force microscope (AFM, Dualscope/RasterscopeC26), and scanning electron microscope (SEM, Hitachi/S4160). Also, quantitative analysis of the thickness of obtained deposits was explored using a Veeco Dektak-3 profiler. For kinetic studies, the zeta potential and mobility of TiO_2 nanoparticles were measured employing a Malvern Zetasizer (3000 HAS). Conductivity measurements of the prepared suspensions were carried out by a WTW conductivity meter (Inolab/Weilheim).

3. RESULTS AND DISCUSSION

3.1. Suspension Preparation Technique. To prepare stable TiO_2-based suspensions which is a prerequisite for the EPD process, dispersing agents such as iodine have been commonly used in organic media.[25] However, considering the toxicity of such additives,[26] we tried to obtain well-dispersed stable TiO_2 suspensions in all mentioned alcohols by applying appropriate preparation techniques without adding any dispersants. The possible mechanisms of charge bearing on the surface of TiO_2 particles in alcoholic media have been investigated in detail elsewhere.[27] This achievement eliminated

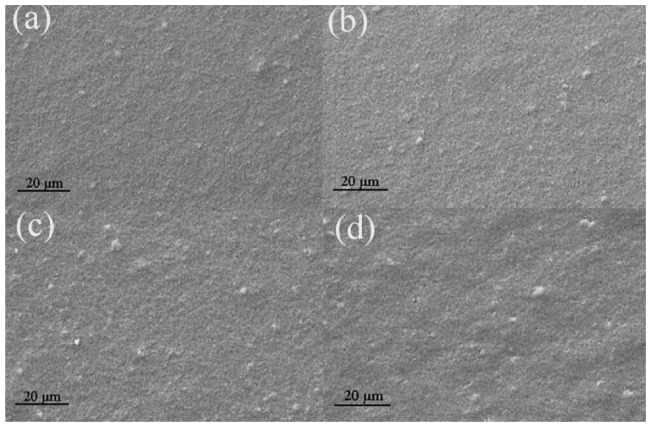

Figure 1. SEM image of layers obtained by the multistep EPD method in methanol (a), ethanol (b), 1-propanol (c), and butanol (d) for 2 g/L suspensions.

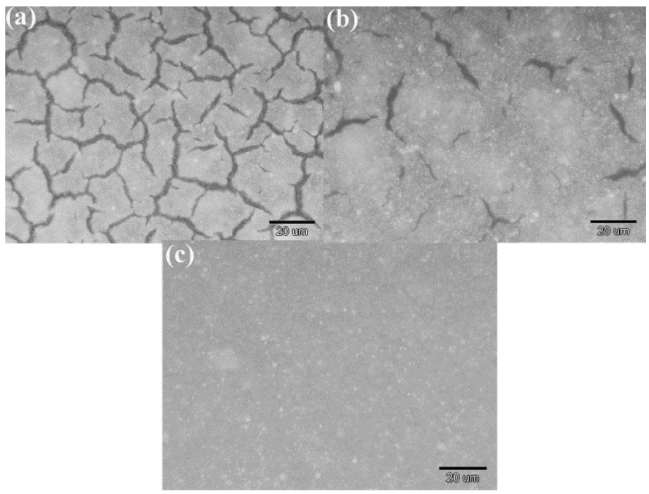

Figure 2. The OM images of the deposition patterns obtained by the single-, two-, and six-step EPD method for TiO_2 nanoparticles in 1-propanol.

dx.doi.org/10.1021/jp306976p | J. Phys. Chem. B 2013, 117, 1731−1737

Table 1. Longest Time Steps during Which Crack-Free Layers Were Obtained in Each Medium

suspension	10 s	20 s	30 s	60 s	120 s
methanol	crack-free	cracked	cracked	cracked	cracked
ethanol	crack-free	crack-free	cracked	cracked	cracked
1-propanol	crack-free	crack-free	crack-free	cracked	cracked
butanol	crack-free	crack-free	crack-free	crack-free	cracked

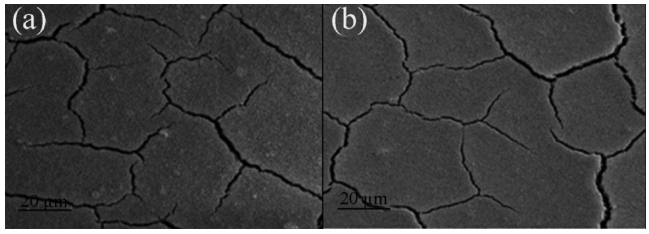

Figure 3. Crack formation across EPD layers formed in (a) methanol (3 g/L) and (b) ethanol (5 g/L).

Table 2. Physical Properties of Solvents[35]

organic medium	absolute viscosity (Pa·s)	dielectric constant	vapor pressure (mmHg)
methanol	0.6	32.6	103
ethanol	1.08	22.4	45.7
1-propanol	1.72	20.1	13.4
butanol	3	18.2	4.6

Table 3. Suspension Parameters Measured in Different Solvents

organic medium	mobility (μmcm/V·s)	zeta potential (mV)
methanol	1.154	24
ethanol	0.379	19.4
1-propanol	0.179	17.3
butanol	0.087	16.2

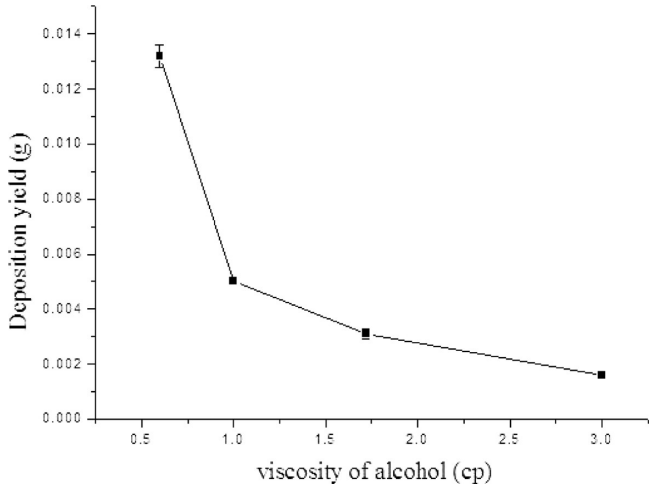

Figure 5. Deposition yield as a function of suspension viscosity in four alcoholic media.

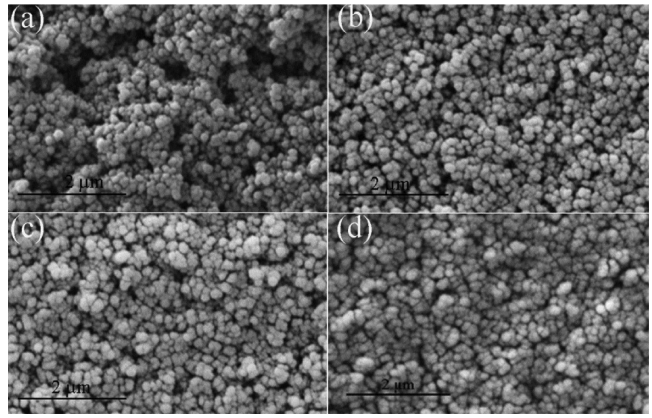

Figure 6. SEM micrograph of EPD layers obtained in methanol (a), ethanol (b), 1-propanol (c), and butanol (d) from 2 g/L suspensions.

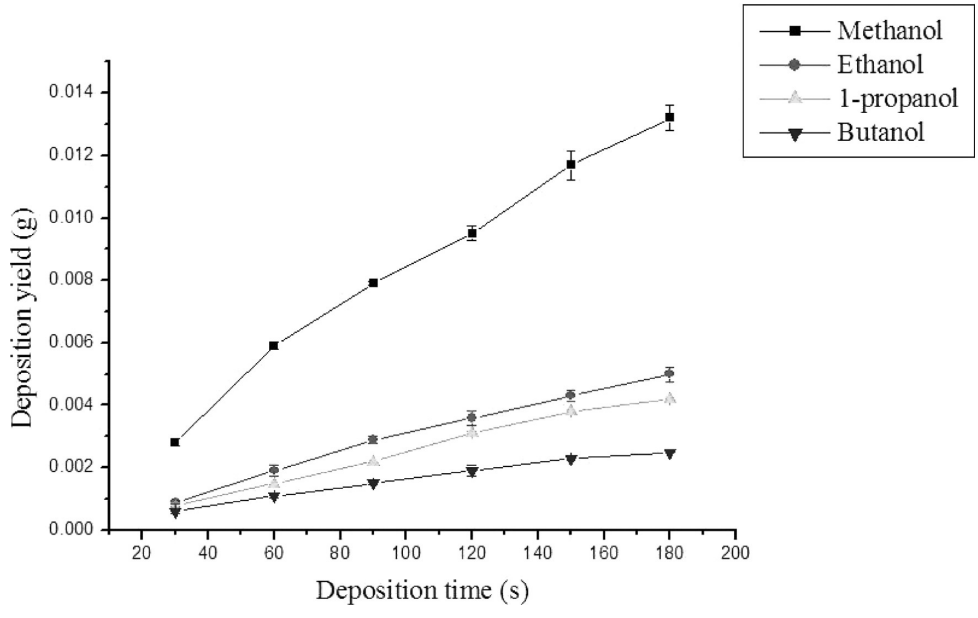

Figure 4. Deposition yield versus time in four organic media for 2 g/L suspensions.

dx.doi.org/10.1021/jp306976p | J. Phys. Chem. B 2013, 117, 1731−1737

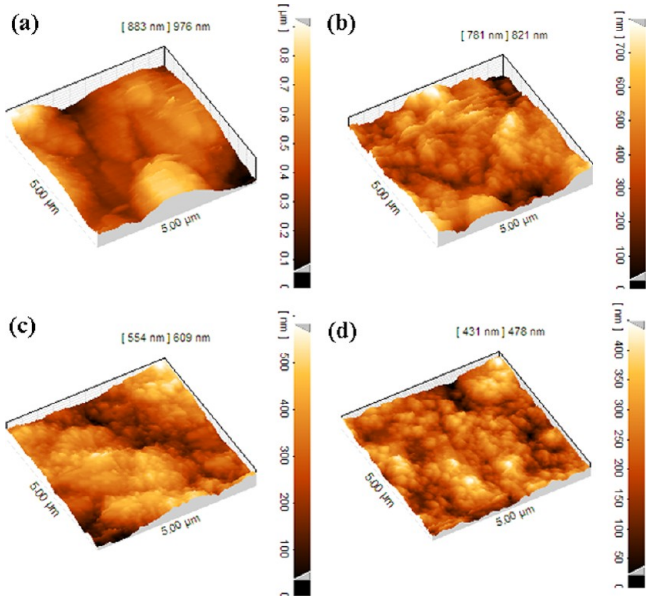

Figure 7. AFM images of EPD layers obtained in methanol (a), ethanol (b), 1-propanol (c), and butanol (d) from 2 g/L suspensions.

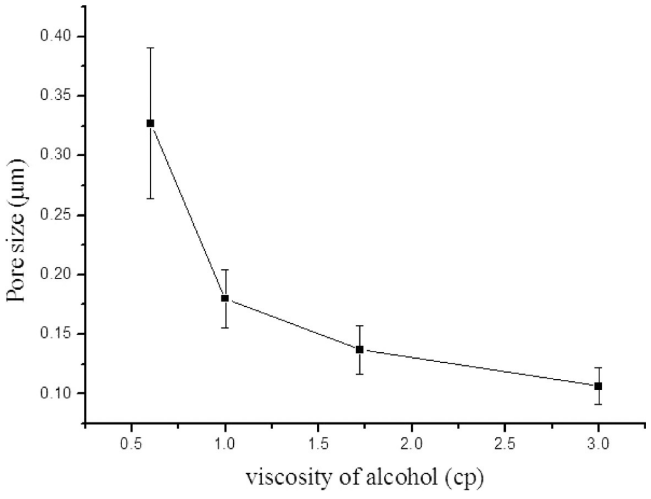

Figure 8. The average size of the pores in EPD layers measured by the image processing technique.

the need to add dispersant, offering us the possibility to focus on inherent characteristics of the medium as responsible for the formation of different microstructures. It must be pointed out that the presence of additive species within the structure of the TiO_2 film could possibly have unexpected detrimental effects on the properties of fabricated devices such as solar cells.[28]

3.2. Multistep EPD Technique. The SEM images of the layers obtained through electrophoretic deposition of TiO_2 nanoparticles in four different organic media (2 g/L suspensions) are depicted in Figure 1. The layers' thickness was measured to be 20 μm using both a Veeco Dektak-3 profiler and the optical microscope image of the film's cross section. This evidence clearly indicates that crack-free layers with a thickness of about 20 μm can be obtained through the application of the multistep deposition technique where TiO_2 layers are alternatively deposited and dried in air.

The first reason behind using the multistep deposition method is that the continuous deposition of TiO_2 nanoparticles was observed to result in the formation of cracks in the case of thick layers. In fact, as the layer is growing thicker during the deposition process, the increased resistance of this nonconductive layer is expected to weaken the electric field force in front of the film, resulting in poor interparticle connections across the depositing layers. As we discussed in our previous study,[6] formation of cracks during the drying step could be attributed to high evaporation rate of solvent as well as lack of compactness within the layer.

Severe cracking of the deposit is illustrated in Figure 2a which is a TiO_2 layer made under continuous deposition from a 4 g/L 1-propanol-based suspension. It is interestingly observed that increasing the deposition process to two steps has limited the formation of cracks (Figure 2b). Figure 2c obviously shows that further increase of deposition steps to six effectively eliminates crack formation across the TiO_2 layer. In this method, a single time step is defined as the longest deposition time in which a crack-free deposit is obtained at constant deposition parameters (voltage, medium). The time step durations obtained for the organic media in the present work are presented in Table 1. Yanagida et al.[29] determined the time step for the formation of crack-free layers of submicrometer TiO_2 in isopropanol to be about 120 s. The high viscosity of isopropanol which results in a lower deposition rate could be the main factor elongating the time required for the formation of a cracked layer. As shown by Table 1, the longest step in the present study was achieved for butanol which is the most viscous media employed.

3.3. Critical Cracking Thickness (CCT) and Concentration Limit. In general, there is a critical cracking thickness (CCT) above which the deposited layer is cracked. A layer that exceeds the CCT value will form an incompact layer structure prone to cracking. Naim et al. reported 10 and 17 μm as the CCT value in pulse direct current (DC) electrophoretic deposition of TiO_2 nanoparticles from an aqueous TiO_2 suspension. In the present work, by applying the multistep deposition technique, we increased the CCT value to 21 μm.[19,30] This indicates that, in addition to basic deposition parameters such as solvent medium, particle size, concentration, and dispersing agent commonly introduced as the variables directly affecting the CCT value, this parameter is also simply controllable through the application of proper EPD technique. In the present study, the CCT values obtained for deposits formed in 2 g/L suspensions of methanol and butanol were determined to be 20 and 24 μm, respectively.

The addition of impurities to the system has also been employed to achieve smooth deposits. Chang et al. applied the multielectrophoresis deposition of TiO_2 nanoparticles in isopropanol and $Mg(NO_3)_2{\cdot}6H_2O$ to prevent crack formation. They decreased the solvent evaporation rate by placing the film in a low-temperature environment which led to successful obtainment of a crack-free layer with a thickness of about 12 μm.[31] However, the multistep EPD technique gave us the chance to prevent crack formation without the introduction of any impurities into the system and with no need to change the temperature.

In addition to the way we carry out the EPD process (single-step or multistep technique), the crack formation phenomenon is also dependent on the concentration of particles within the suspension. In order to investigate the effect of suspension concentration on the incidence of cracks across the layer, electrophoretic deposition of TiO_2 nanoparticles in four organic media—methanol, ethanol, 1-propanol, and butanol—was performed in 1−8 g/L suspensions. In multistep

dx.doi.org/10.1021/jp306976p | J. Phys. Chem. B 2013, 117, 1731−1737

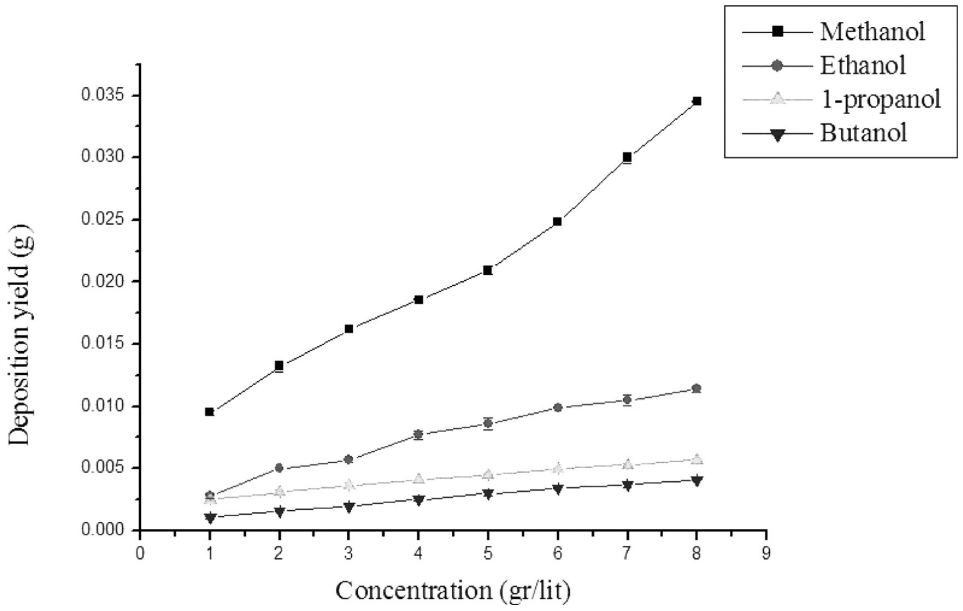

Figure 9. Deposition yield versus concentration in four organic suspensions.

electrophoretic deposition of TiO_2 nanoparticles in methanol and ethanol, a threshold concentration was detected below which no cracks were formed. As illustrated in Figure 3, the threshold values for methanol and ethanol are 3 and 5 g/L, respectively. This figure shows that the fabricated films have been severely cracked after being dried at 150 °C in air. However, in heavier alcohols, 1-propanol and butanol, no cracks were observed even at concentrations as high as 8 g/L. In brief, the critical cracking concentration (CCC) of TiO_2 layers formed in more viscous alcohols was found to be higher in comparison with the layers obtained in less viscous media.

As mentioned above, in contrast with methanol and ethanol, the electrophoretic deposition of TiO_2 nanoparticles from 1-propanol- and butanol-based suspensions was successfully carried out without crack formation even for high powder concentrations up to 8 g/L. In fact, by using more viscous media, we increased the critical cracking concentration for the deposition of TiO_2 nanoparticles in organic media from 4 g/L (for methanol and ethanol) to values higher than 8 g/L (for 1-propanol and butanol). In a previous study, Naim et al.[19] dealt with the effect of particle population on the quality of deposited layers with a different approach. They successfully increased the CCT for electrophoretically deposited TiO_2 films by decreasing the concentration of particles within the suspension. However, in the present work, we showed that by employing vehicles of higher viscosity it is possible to preserve the CCT values obtained in less viscous media with no need to decrease the colloidal concentration of the suspension. As an example, for a 7 g/L suspension of TiO_2 in methanol or ethanol, cracks were observed to form even at extremely short durations (below 10 s). However, by turning to more viscous media such as 1-propanol and butanol for the same concentration of TiO_2 nanoparticles, thick films with a thickness of over 20 μm were obtained without the formation of cracks. In other words, for 7 g/L TiO_2 suspensions in organic media, the CCT can be increased through the application of more viscous vehicles.

3.4. Crack Formation Mechanism. Formation and propagation of microcracks across electrophoretically deposited TiO_2-based layers could be first attributed to the high evaporation rate of methanol and ethanol (Table 2) as well as the shrinkage of the deposit as a result of solvent evaporation. When coatings containing suspended submicrometer-sized colloidal particles are dried on a substrate, the evaporation of solvent concentrates the particles into a close-packed array where the liquid at the top of the layer exerts a compressive capillary force on the particle network. In this case, since the layer binds to the substrate and resists transverse deformation, transverse tensile stresses are created and lead to crack formation in the case of hard particles.[30] This mechanism indicates that the liquid trapped within the layer during the deposition process plays an important role in the capillary tension and subsequent cracking.

On the basis of the relation reported by Tirumkudulu and Russel,[32] the critical stress (σ_c) for the initiation of an isolated crack is directly proportional to the fraction volume of particles. In other words, as the amount of fluid trapped within the layer during deposition is decreased, the volume fraction of particles is increased. In such conditions, it is expected that the critical stress for crack initiation be enhanced, maximizing the chance of obtaining a crack-free microstructure. In the present work, the application of the multistep EPD technique reduces the total trapped liquid within the deposit because in each step some of the liquid is evaporated during drying. On the other hand, when the whole deposition is carried out in a single step, severe liquid trapping in the deposited layer reduces the volume fraction of particles, giving rise to a significant shrinkage across the layer which results in the formation of cracks. The formation of cracks could have detrimental effects on the performance of fabricated devices. For example, in DSSCs, these defects would cause recombination of charge carriers, and subsequently lower the current density and the energy conversion efficiency.[33]

3.5. Microstuctral Studies and Deposition Kinetics. In order to analyze the different concentration thresholds observed for the mentioned alcoholic media, deposition kinetics in these four media was investigated. According to the presented data in Table 2, methanol and ethanol are less viscous media with relatively higher dissociation power compared with 1-propanol and butanol. Hence, according to Smoluchowski's equation (eq 1), it is expected that TiO_2

dx.doi.org/10.1021/jp306976p | J. Phys. Chem. B 2013, 117, 1731−1737

nanoparticles' electrophoretic mobility in ethanol and methanol is larger than in heavier alcohols.[18]

$$\mu = \frac{2}{3}\frac{\varepsilon\varepsilon_0\zeta(f(ka)}{\eta} \quad (1)$$

In this equation, ε is the permittivity of the vacuum, ε_0 is the relative permittivity of the solvent, η is the solvent viscosity, ζ is the zeta potential, and $f(kr)$ is the Henry coefficient.

The higher mobility of TiO_2 nanoparticles in less viscous media is confirmed by zeta potential results presented in Table 3 where the particle mobility in methanol is about 6 and 13 times greater than that obtained in 1-propanol and butanol, respectively. Similar results were presented by Panigrahi et al.[21] where they reported a high deposition rate and an uneven microstructure for doped ceria micropowder in ethanol. In contrast, the deposition rate in butanol was small and smooth deposits were obtained. In order to compare the deposition rate of TiO_2 nanoparticles in the four mentioned media, the deposited weight was drawn as a function of time for 30 s intervals. The results which are illustrated in Figure 4 indicate that the rate of deposition decreases as the viscosity increases which is in accordance with mobility and zeta potential results. These data are summarized in Figure 5, where the deposition yield for 2 g/L suspensions is shown as a function of the viscosity (Table 2). At low viscosities and high deposition rates, the rapid attraction of suspended particles toward the oppositely charged electrode gives them little chance to be assembled in a sufficiently packed structure. However, when the particles have enough time to approach the electrode surface, it is possible for them to assemble in more compact configurations.

The surface microstructure of as-prepared TiO_2 films obtained in the four organic media was analyzed by SEM. As shown in Figure 6, the layers formed in ethanol and methanol (Figure 6a and b) appeared to be more porous containing large pores within their structures. Meanwhile, the deposits obtained in heavier alcohols, 1-propanol and butanol, are comparatively more compact exhibiting a uniform structure. These results are also confirmed by atomic force microscope (AFM) studies on deposits formed in methanol, ethanol, 1-propanol, and butanol. It is clearly shown by Figure 7 that an increase in the organic medium viscosity (from part a to part d) is accompanied by an evident reduction in the surface roughness of the deposited layer.

In addition to high deposition rate, the formation of porous structures for TiO_2 deposits could also be attributed to particle agglomeration and the fact that it is more difficult for large aggregates to deposit in a close-packed structure compared to the smaller ones. According to the DLVO theory, two adjacent colloid particles attract each other due to van der Waals forces and simultaneously repel by repulsive electrostatic forces because of their surface charge. Since van der Waals forces are weak short-range forces, if two given particles in a liquid are going to form an aggregate, they need to come sufficiently close to each other so that attractive van der Waals forces can link the particles together and create a larger aggregate. On the basis of this fact, for two given suspensions of the same concentration, particle collisions resulting in agglomeration would be dependent on how freely they can migrate in the media. The diffusion coefficient of suspended particles in a given medium is described as[34]

$$D = \frac{kT}{6\pi\eta a} \quad (2)$$

where D is the diffusion coefficient, k is the Boltzmann constant, and η and T are the fluid viscosity and the temperature, respectively. On the basis of the above discussion and considering the inverse relation between diffusion coefficient and fluid viscosity (eq 2), it can be concluded that in viscous media it takes particles/aggregates more time to reach close enough to form larger agglomerates through attractive van der Waals forces. As a result, uniform and crack-free deposits are expected to form in heavier alcohols as we reported in a recent study for ZnO nanoparticles under the application of low frequency alternating electric fields.[22]

The lack of compactness due to substantially higher deposition rates in less viscous media is expected to facilitate the liquid trapping within the depositing film. In fact, at high deposition rates, the interparticle spacing across the layer is higher and this space is mostly filled with the surrounding liquid. By reducing the deposition rate at higher viscosities, the TiO_2 nanoparticles are given the opportunity to find a more energetically stable position on the substrate, improving the compactness of the layer. In this case, the volume fraction of the particles in the microstructure of the deposit will improve, leaving behind much less space for the liquid to trap.

In the present work, an image analysis technique was employed using the ImageJ software (1.38x) to measure the average diameter of the pores taking 10 random pores on the SEM images with a magnification of 20 k. The pore sizes obtained for EPD deposits (at 2 g/L) were 327, 164, 137, and 106 nm in methanol, ethanol, 1-propanol, and butanol, respectively. The image analysis porosimetry clearly shows that the compactness of the electrophoretically deposited TiO_2 layers is increased as a function of the viscosity of the alcoholic media (Table 2). This trend is depicted in Figure 8. The important point about Figure 8 is the remarkable difference in standard deviation value obtained for the pore size of the layer formed in methanol compared to the other three media. This broad range of pore size is attributed to the high deposition rate in methanol which results in the mass movement of high speed particles toward the electrode. In this condition, the depositing particles lose their opportunity to choose suitable positions on the electrode surface and consequently form a nonuniform porous pattern on the substrate.

Electrophoretic deposition of TiO_2 nanoparticles from four organic media with different rheological and dielectric properties showed that more uniform and compact layers can be obtained in 1-propanol and butanol due to higher viscosity and moderate deposition rates compared to ethanol and methanol. In addition, it was found that EPD from supensions prepared in less viscous media suffers from some limitations in concentration so that deposits formed in 4 g/L ethanol and methanol-based suspensions were cracked after drying. However, such limitations were not observed in 1-propanol and butanol. Thus, if our goal is to obtain uniform crack-free EPD layers with sufficient interconnection between particles and at the same time maintain fast enough deposition rates, heavy alcohols at high concentrations (here, up to 8 g/L) can be suitable choices. It was observed that by increasing the suspension concentration in butanol from 4 to 8 g/L the deposition yield increased from 0.0025 to 0.0041 g (Figure 9). The same trend was observed in 1-propanol. Hence, slower deposition rates in viscous media

dx.doi.org/10.1021/jp306976p | J. Phys. Chem. B 2013, 117, 1731−1737

can be compensated by increasing the concentration of TiO_2 nanopowder (Figure 9).

4. CONCLUSION

We obtained crack-free layers with a thickness of about 20 μm through the application of multistep deposition electrophoresis in four alcoholic media. It was observed that in less viscous alcohols, methanol and ethanol, there was a critical concentration (3 and 5 g/L) above which the layers cracked. However, by increasing the viscosity of the media using heavier alcohols, crack formation was not observed even at concentrations as high as 8 g/L. In this case, the low deposition rate of TiO_2 nanoparticles in more viscous media was held responsible for their substantial resistance to crack formation even at high concentrations. Increasing the concentration in heavier alcohols has given us a valuable chance to obtain crack-free deposits at shorter EPD durations.

AUTHOR INFORMATION

Corresponding Author

*Phone: +98 912 5398676. E-mail: babakraissi@yahoo.com.

Notes

The authors declare no competing financial interest.

REFERENCES

(1) Nahar, M. S.; Zhang, J.; Hasegawa, K.; Kagaya, S.; Kuroda, S. *Mater. Sci. Semicond. Process.* **2009**, *12*, 168−174.
(2) Radecka, M.; Rekas, M.; Trenczek-Zajac, A.; Zakrzewska, K. *J. Power Sources* **2008**, *181*, 46−55.
(3) Liu, Y.; Lü, C.; Li, M.; Zhang, L.; Yang, B. *Colloids Surf., A* **2008**, *328*, 67−72.
(4) Lee, M.-K.; Lee, H.-C.; Hsu, C.-M. *Mater. Sci. Semicond. Process.* **2007**, *10*, 61−67.
(5) Zhang, L.; Zhu, Y.; He, Y.; Li, W.; Sun, H. *Appl. Catal., B* **2003**, *40*, 287−292.
(6) Fateminia, S. M. A.; Yazdani-Rad, R.; Ebadzadeh, T.; Ghashghai, S. *Appl. Surf. Sci.* **2011**, *257*, 8500−8505.
(7) Mohammadi, M. R.; Fray, D. J.; Cordero-Cabrera, M. C. *Sens. Actuators, B* **2007**, *124*, 74−83.
(8) Natsuhara, H.; Matsumoto, K.; Yoshida, N.; Itoh, T.; Nonomura, S.; Fukawa, M.; Sato, K. *Sol. Energy Mater. Sol. Cells* **2006**, *90*, 2867−2880.
(9) Santillán, M. J.; Quaranta, N.; Membrives, F.; Roether, J A.; Boccaccini, A. R. *Key Eng. Mater.* **2009**, *412*, 189−194.
(10) Yu, X.; Shen, Z. *Vacuum* **2011**, *85*, 1026−1031.
(11) Segota, S.; Curkovic, L.; Ljubas, D.; Svetlicic, V.; Houra, I. F.; Tomasic, N. *Ceram. Int.* **2011**, *37*, 1153−1160.
(12) Nang Dinh, N.; Minh Quyen, N.; Chung, D. N.; Zikova, M.; Truong, V.-V. *Sol. Energy Mater. Sol. Cells* **2011**, *95*, 618−623.
(13) Fan, K.; Liu, M.; Peng, T.; Ma, L.; Dai, K. *Renewable Energy* **2010**, *35*, 555−561.
(14) Tomaszek, R.; Znamirowski, Z.; Pawlowski, L.; Zdanowski, J. *Vacuum* **2007**, *81*, 1278−1282.
(15) Suisalu, A.; Aarik, J.; Mändar, H.; Sildos, I. *Thin Solid Films* **1998**, *336*, 295−298.
(16) Jung, S.-C.; Kim, S.-J.; Imaishi, N.; Cho, Y.-I. *Appl. Catal., B* **2005**, *55*, 253−257.
(17) Sarkar, P.; Nicholson, P. S. *J. Am. Ceram. Soc.* **1996**, *79*, 1987−2002.
(18) Van der Biest, O. O.; Vandeperre, L. J. *Annu. Rev. Mater. Sci.* **1999**, *29*, 327−352.
(19) Naim, M. N.; Iijima, M.; Kamiya, H.; Lenggoro, I. W. *Colloids Surf., A* **2010**, *360*, 13−19.
(20) Uchikoshi, T.; Ozawa, K.; Hatton, B. D.; Sakka, Y. *J. Mater. Res.* **2001**, *16*, 321−324.
(21) Panigrahi, S.; Bhattacharjee, S.; Besra, L.; Singh, B. P.; Sinha, S. P. *J. Eur. Ceram. Soc.* **2010**, *30*, 1097−1103.
(22) Ghashghaie, S.; Marzbanrad, E.; Raissi Dehkordi, B. *J. Am. Ceram. Soc.* **2011**, no−no.
(23) Dor, S.; Rühle, S.; Ofir, A.; Adler, M.; Grinis, L.; Zaban, A. *Colloids Surf., A* **2009**, *342*, 70−75.
(24) Grinis, L.; Dor, S.; Ofir, A.; Zaban, A. *J. Photochem. Photobiol., A* **2008**, *198*, 52−59.
(25) Boccaccini, A. R.; Rossetti, M.; Roether, J. A.; Sharif Zein, S. H.; Ferraris, M. *Constr. Build. Mater.* **2009**, *23*, 2554−2558.
(26) Pennington, J. A. *J. Am. Diet. Assoc.* **1990**, *90*, 1571−81.
(27) Radice, S.; Bradbury, C. R.; Michler, J.; Mischler, S. *J. Eur. Ceram. Soc.* **2010**, *30*, 1079−1088.
(28) Pimanpang, S.; Maiaugree, W.; Jarernboon, W.; Maensiri, S.; Amornkitbamrung, V. *Synth. Met.* **2009**, *159*, 1996−2000.
(29) Yanagida, S.; Nakajima, A.; Kameshima, Y.; Yoshida, N.; Watanabe, T.; Okada, K. *Mater. Res. Bull.* **2005**, *40*, 1335−1344.
(30) Singh, K. B.; Tirumkudulu, M. S. *Phys. Rev. Lett.* **2007**, *98*, 218302.
(31) Chang, H.; Su, H.-T.; Chen, W.-A.; David Huang, K.; Chien, S.-H.; Chen, S.-L.; Chen, C.-C. *Sol. Energy* **2010**, *84*, 130−136.
(32) Tirumkudulu, M. S.; Russel, W. B. *Langmuir* **2004**, *20*, 2947−2961.
(33) Jarernboon, W.; Pimanpang, S.; Maensiri, S.; Swatsitang, E.; Amornkitbamrung, V. *Thin Solid Films* **2009**, *517*, 4663−4667.
(34) Einstein, A. *Investigations on the Theory of Brownian Movement*; Dover: New York, 1956.
(35) Smallwood, I. M. *Handbook of organic solvent properties*; Arnold, Halsted Press: London, 1996.